JACS
JOURNAL OF THE AMERICAN CHEMICAL SOCIETY
Communication
pubs.acs.org/JACS

Strategy for "Detoxification" of a Cancer-Derived Histone Mutant Based on Mapping Its Interaction with the Methyltransferase PRC2

Zachary Z. Brown,[†,∥] Manuel M. Müller,[†,∥] Siddhant U. Jain,[‡] C. David Allis,[§] Peter W. Lewis,[‡] and Tom W. Muir*[,†]

[†]Department of Chemistry, Princeton University, Princeton, New Jersey 08544, United States
[‡]Epigenetics Theme, Wisconsin Institute for Discovery, University of Wisconsin, Madison, Wisconsin 53715, United States
[§]Laboratory of Chromatin Biology & Epigenetics, The Rockefeller University, New York, New York 10065, United States

Supporting Information

ABSTRACT: The histone methyltransferase PRC2 plays a central role in genomic stability and cellular development. Consequently, its misregulation has been implicated in several cancers. Recent work has shown that a histone H3 mutant, where the PRC2 substrate residue Lys27 is replaced by methionine, is also associated with cancer phenotypes and functions as an inhibitor of PRC2. Here we investigate the mechanism of this PRC2 inhibition through kinetic studies and photo-cross-linking. Efficient inhibition is dependent on (1) hydrophobic lysine isosteres blocking the active site, (2) proximal residues, and (3) the H3 tail forming extensive contacts with the EZH2 subunit of PRC2. We further show that naturally occurring post-translational modifications of the same H3 tail, both proximal and distal to K27M, can greatly diminish the inhibition of PRC2. These results suggest that this potent gain of function mutation may be "detoxified" by modulating alternate chromatin modification pathways.

Covalent modifications of chromatin facilitate the dynamic organization of eukaryotic genomes and fine-tuning of transcriptional outputs.[1] Proteins that install or remove functional groups, or specifically recognize modified chromatin, mediate downstream biochemical processes and are essential for cell growth, homeostasis, and lineage commitment. Consequently, misregulation of chromatin-associated proteins is frequently correlated with disease states. In particular, mutations altering EZH2, the catalytic subunit of the polycomb repressor complex 2 (PRC2), are often found in cancers where they interfere with PRC2's role in gene silencing.[3] At the molecular level, PRC2 functions by methylating Lys27 within the N-terminal tail region of histone H3.[4] Intriguingly, Lys27 is frequently mutated to methionine (H3K27M) in a subpopulation of histone H3 in pediatric glioblastomas.[5,6] Despite representing only a few percent of the total H3 pool in glioma cells, H3K27M is able to strongly diminish global levels of H3K27 methylation by directly binding to PRC2.[7−9] Paradoxically though, an analysis of the chromatin landscape in K27M-carrying tumor tissues revealed that small regions of the genome escaped inhibition.[8,9] These islands of K27me3 probably contribute to the mechanism of K27M-mediated pathogenesis, but how certain regions overcome the inhibitory effects of the K27M mutation is currently unknown. Finding a way to restore K27me3 to the rest of the genome would be a strategy to mitigate the consequences of this deleterious mutation. The intricacies of PRC2 regulation, along with the frequency by which its activity is perturbed in human pathologies, create urgency in understanding how substrates and inhibitors interact with this multisubunit enzyme complex. Here we present a detailed biochemical investigation into how PRC2 recognizes the mutated H3 tail. A comprehensive structure−activity relationship (SAR) analysis of the H3 tail revealed key orthosteric and allosteric contributions to binding and recognition by PRC2. Photo-cross-linking studies served to identify the subunits of PRC2 responsible for H3 tail recognition. Finally, we show that inhibition of PRC2 can be significantly diminished by post-translational modifications (PTMs) on the same H3 peptide, providing a potential mechanism for how these cancer-derived H3 mutations might be overcome.

We began by characterizing the inhibition of PRC2 activity by H3K27M mutant mononucleosomes. Wild-type and H3K27M nucleosomes were assembled using purified recombinant histone proteins and a strong nucleosome positioning DNA sequence (Widom-601).[10] Methyltransferase activity was measured by scintillation counting upon incubation of wild-type nucleosome substrates with ^{3}H-containing *S*-adenosylmethionine (^{3}H-SAM) in the presence of PRC2, purified from HeLa cells (Figure 1A, see Supporting Information for details). In agreement with previous measurements,[11] an apparent K_m value ($K_{m,app}$) of 67 ± 26 nM was obtained for the wild-type nucleosome substrate (Figure S1). H3K27M-containing nucleosomes inhibited PRC2 with K_I = 2.1 ± 0.9 nM. Under these conditions, the mechanism of inhibition appears competitive (vs mononucleosome substrates), indicated by a linear dependence of the K27M IC_{50} values on the concentration of substrates (Figure 1B).[12,13] In contrast, the IC_{50} value of K27M-nucleosomes was independent of the concentration of SAM, consistent with noncompetitive inhibition (vs SAM, Figure S1C). These values are in agreement with the strong inhibition of PRC2 activity observed in tumor tissues, despite the overwhelming excess of wild-type histones over mutant congeners. While H3K27M mononucleosomes are remarkably potent inhibitors, with a molecular mass of almost 200 kDa, they have many sites of potential interaction with PRC2. Therefore,

Received: June 17, 2014
Published: September 2, 2014

   dx.doi.org/10.1021/ja5060934 | J. Am. Chem. Soc. 2014, 136, 13498−13501

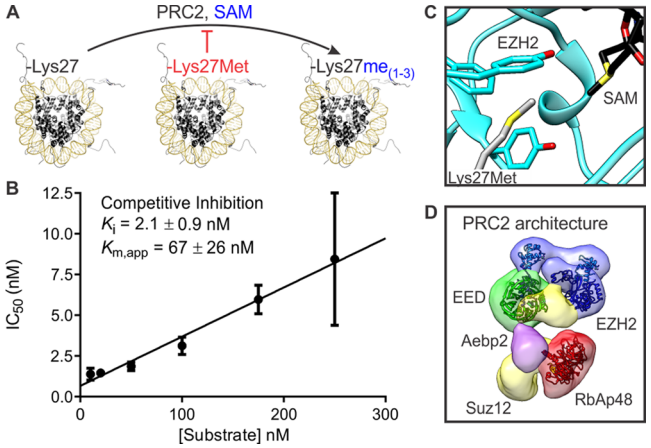

Figure 1. Model for PRC2 activity and inhibition. (A) Schematic representation of PRC2 activity. (B) Cheng–Prusoff analysis of the mechanism of PRC2 inhibition by K27M. IC_{50} values were determined at varying concentrations of unmodified mononucleosome substrates. (C) Homology model of the EZH2 active site (cyan) bound by a methionine residue (white). The cofactor SAM is depicted in black. (D) Molecular architecture of PRC2; adapted from Ciferri et al. (EMD-2236).[2]

we sought to dissect the various contributions of allosteric and orthosteric inhibitor binding to PRC2.

SET domain methyltransferases, including EZH2, bind the hydrophobic (alkyl) portion of the lysine side chain in an aromatic cage (Figure 1C).[14] Additionally, the active site utilizes cation–π interactions to recognize and distinguish its substrates: unmethylated and mono- and dimethylated lysine 27. A hydrogen-bond donor deep in the pocket assists in aligning the ε-amine for nucleophilic attack on the methyl donor SAM. Methionine and to a lesser extent isoleucine are able to bind in this pocket and inhibit PRC2 *in vivo*, suggesting that recognition of a hydrophobic moiety is a primary factor for potent inhibition.[7] Further *in vitro* work established norleucine (Nle) as a more potent methionine isostere.[7] To gain more insight into the steric and electronic factors governing inhibitor binding to the EZH2 active site, we designed a series of short peptide constructs (residues 23–34 of the H3 variant H3.3) that differed only in residue 27 (Table 1). Each peptide (50 μM) was assayed for inhibition of methyltransferase activity using a scintillation assay containing PRC2, ^{3}H-SAM, and a substrate peptide (20 μM). Under these conditions, the K27M peptide (**1**) inhibited methyltransferase activity by 53% ± 7%. Norleucine (**2**) as well as (*S*)-aminoheptanoic acid (**3**) exhibited complete inhibition. In a full IC_{50} determination, peptides **1** and **2** had respective IC_{50} values of 56 ± 7 and 3.3 ± 0.5 μM (Figure S2A). Shortening the carbon chain by one methylene group to norvaline (peptide **5**) provided a modest loss in activity. Some branching aliphatic side chains (peptides **6** and **9**) may be tolerated, although provide no improvement over the more potent straight chain aliphatics (**5** and **2**, respectively). Other branching geometries (**7** and **8**), as well as the peptide which included (*R*)-aminoheptanoic acid (**4**), did not provide measurable inhibition.

We further sought to assess the effect of heteroatom substitution within the side-chain. To probe whether cation–π interactions could be harnessed with various lysine analogs, we synthesized several diamine building blocks (Table 1). However, the corresponding series of peptides showed little to no inhibition (peptides **10**–**15**). We therefore resorted to less polar heteroatom containing side-chains. Conversion of the thioether moiety of K27M to an ether (peptide **16**) resulted in modest loss of inhibition. Oxidation of methionine to the sulfoxide (peptide **17**) abolished inhibition. Trifluoro-methionine (peptide **18**) inhibited PRC2 substantially better than methionine (IC_{50} of 11 ± 2 μM for **18** vs 56 ± 7 μM for **1**, Figure S2A). Methionine analogs with diverse steric properties (peptides **20**–**25**) were generated through chemoselective alkylation of thiols at the peptide level (Scheme S2). Both cysteine and homocysteine were derivatized with various π-electron-containing electrophiles. Although several of the peptides (**21**–**24**) provided measurable inhibition, none were a significant improvement over the aliphatic entries **2** or **3**. Thus, the EZH2 active site binds strongly to linear, hydrophobic side chains with little tolerance to extra steric bulk and polar groups.

To probe whether distal regions of the H3 tail are also recognized by the PRC2 complex, we prepared a range of truncated H3 peptides bearing norleucine at position 27 (Figure 2A). Peptide **26**, encompassing residues 1–37 was left with a free N-terminus to reflect the biologically prevalent form of the H3 tail, while truncated constructs were acetylated at their N-termini. IC_{50} values were calculated from methyltransferase assays using

Table 1. SAR of PRC2 Inhibition by H3.3 Peptides (residues 23–34) Bearing Substitutions at the Orthosteric Residue K27[a]

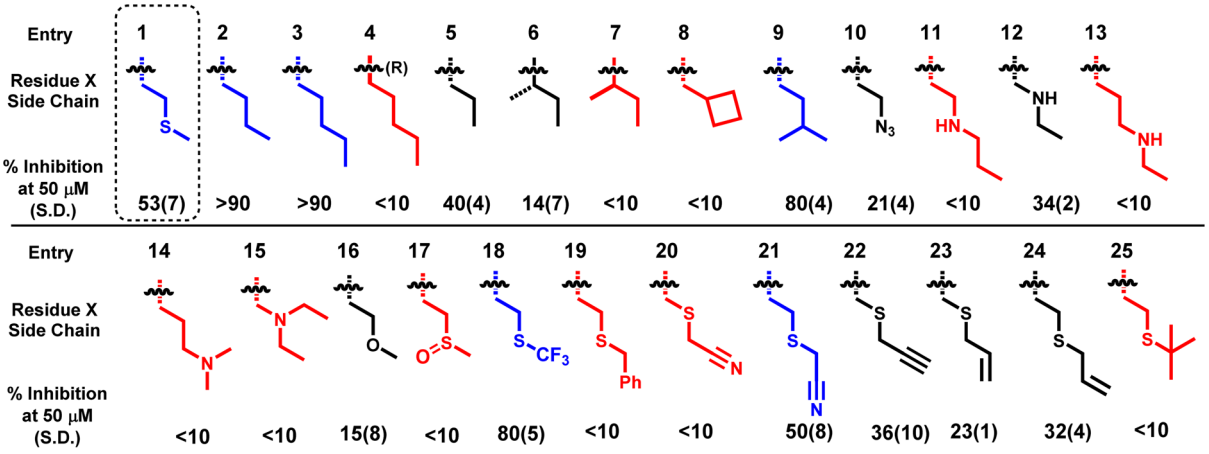

[a]Peptide sequence: KAARXSAPSTGG; where X is varied as indicated. The cancer-derived methionine mutant is boxed. Blue indicates >50% inhibition of PRC2 activity; black denotes an intermediate level of inhibition, red indicates no measurable inhibition. S.D. is one standard deviation.

dx.doi.org/10.1021/ja5060934 | J. Am. Chem. Soc. 2014, 136, 13498–13501

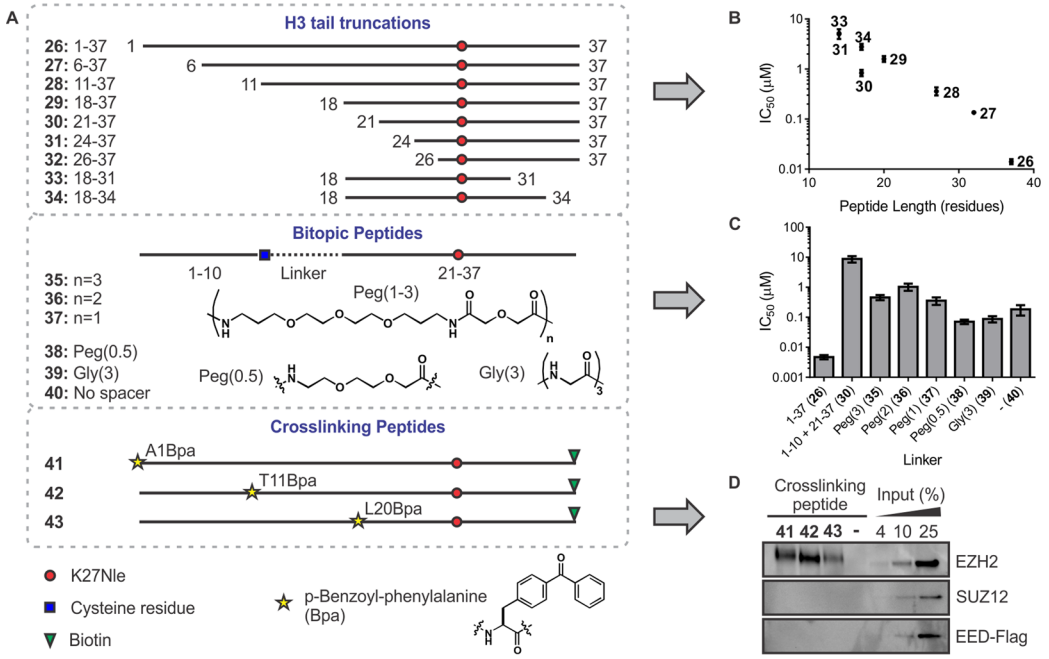

Figure 2. Molecular recognition of the H3 tail by PRC2. (A) Schematic view of truncated H3 tail segments used in (B), bitopic constructs used in (C), and the cross-linking constructs used in (D). Solid lines indicate peptide segments; red dots indicate the orthosteric inhibitor residue, Nle; dotted lines represent artificial linkers; blue squares represent a cysteine residue; yellow stars a Bpa residue; green triangles a biotin moiety. (B) Residues along the entire H3 tail contribute to PRC2 binding. IC_{50} values were determined for peptides **26**–**34** and plotted as a function of peptide length; $n = 2$–3, error of the fit is indicated. (C) PRC2 binds the H3 tail in a compact fashion. IC_{50} values were determined for indicated peptides; $n = 2$–3, error of the fit is indicated. (D) EZH2 engages the entire H3 tail. PRC2 was photo-cross-linked with the indicated peptides. Cross-linked samples were enriched by streptavidin pull-down and detected by Western blot.

H3(23–34) peptide substrates (Figure 2B). In agreement with previous results, a peptide encompassing residues 18–37 (**29**) displayed an $IC_{50} = 1.6\ \mu M$.[7] Truncations of this construct lead to a small decrease (peptides **31**, **33**, **34**) or even a modest increase (peptide **30**) in inhibitor potency. Excessive shortening of the peptide (**32**) abolished measurable inhibition. In contrast, longer peptide constructs bind more strongly to PRC2. Indeed, the full length tail H3(1–37)K27Nle (peptide **26**) potently inhibits methylation of both peptide and mononucleosome substrates (Figures 2B and S2B), the latter with an $IC_{50} = 4.7 \pm 1.5$ nM which rivals the potency of H3K27M nucleosomes ($IC_{50} = 2.6 \pm 0.5$ nM). The steady increase in H3 tail binding as a function of peptide length suggests that PRC2 engages residues along the entire length of the histone tail (Figure 2B). In particular, residues surrounding Lys27 are critical, and the N-terminal 10 residues contribute substantially to inhibition. As peptides **28** (residues 11–37) and **30** (residues 21–37) display similar potency, intervening residues appear to contribute little binding energy.

To investigate whether the binding of the H3 tail to PRC2 is bivalent in nature, i.e., involving residues 1–10 and 21–37, we designed a series of bitopic peptide constructs that encompassed these two segments (Figure 2A). Polyethylene glycol chains of various lengths (compounds **35**–**38**), as well as a Gly_3 peptide (**39**) were used as conformationally flexible, yet defined linkers between the two peptide segments. In a methyltransferase assay which used mononucleosomes as substrates, we found that bitopic display of H3(1–10) and H3(21–37) is favorable compared to adding both peptides in *trans* (Figure 2C). Moreover, short, flexible linkers (**38**, **39**) outperformed longer linkers (**35**–**37**) and the zero-length linker (**40**). The IC_{50} for compound **38** was found to be 71 nM (Figure S2B), only a 15-fold loss of potency from the full length 1–37 peptide (IC_{50} of 4.7 nM). These results imply a compact binding model for the two distal H3 tail segments.

We next analyzed the trajectory of H3 binding to PRC2 through a cross-linking approach. *p*-Benzoyl-phenylalanine (Bpa) residues were strategically placed within the H3 tail (Figure 2A) at positions 1 (**41**), 11 (**42**), and 20 (**43**), complementing previous experiments[7] with photo-cross-linkers installed at residues 27 and 31 which showed that this region of the H3 tail specifically interacts with the EZH2 subunit. Peptides **41**–**43** proved to be potent inhibitors of PRC2 (Figure S3A). PRC2 subunits (Figure 1D) interacting with the distinct H3 sites were identified upon cross-linking based on either the mobility of the cross-linked species as judged by SDS-PAGE (Figure S3B) or upon streptavidin pulldown followed by Western blot for specific PRC2 components (Figure 2D). All cross-linked species comigrate with EZH2 (Figure S3B), and EZH2 is the sole subunit identified upon isolation of cross-linked products (Figure 2D). As expected, the addition of wild-type mononucleosome reduces the cross-linking signal by competing for PRC2 binding (Figure S3B). Taken together with the previous cross-linking studies,[7] these results provide a map of the interaction of PRC2 with the H3 tail containing the cancer-derived K27M mutant. EZH2 engulfs the entire mutant H3 tail, presumably in a compact binding orientation, with key contributions from sites proximal to residue 27 and at the N-terminus.

Through its accessory subunits, PRC2 is able to precisely sense chromatin states and integrate such signals into its methyltransferase activity output.[15] For instance, PRC2 is subject to a positive feedback loop where K27me3 modifications allosterically activate EZH2 through the EED subunit.[16] In addition, trimethylation of Lys4 of H3—a PTM associated with active chromatin regions—diminishes PRC2 activity.[17] We therefore

dx.doi.org/10.1021/ja5060934 | J. Am. Chem. Soc. 2014, 136, 13498–13501

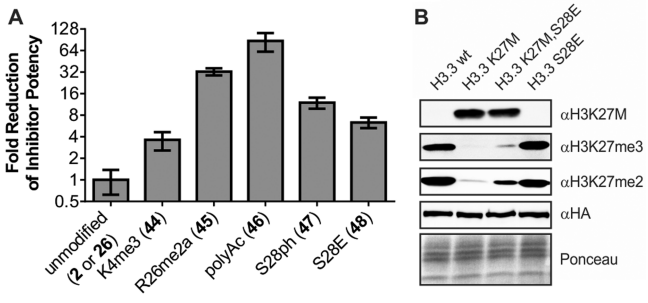

Figure 3. Histone PTMs can detoxify K27M mutants. (A) Reduction of Lys27Nle-dependent inhibition of PRC2 activity by PTMs *in vitro*. (B) Immunoblots of whole-cell extract from lentivirus-transduced HEK293T cells expressing the indicated HA-tagged H3.3 transgenes. The phosphorylation mimic S28E diminishes K27M-dependent PRC2 inhibition *in vivo*.

hypothesized that PRC2 inhibition may be similarly affected by PTMs occurring at binding hotspots. To test this idea, we synthesized peptides containing known activating PTMs within H3. Trimethylation at Lys4 (peptide **44**) reduced inhibitor potency ~4-fold, whereas asymmetric dimethylation at Arg26 (peptide **45**)[18] diminished inhibition ~30-fold (Figures 3A, S4). Polyacetylation of Lys27Nle inhibitor constructs (peptide **46**, acetylated on Lys residues 9, 14, 18, and 23) dramatically impaired Prc2 inhibition, in this case over 80-fold. Notably, K27M nucleosomes are readily acetylated by the histone acetyltransferase p300 (Figure S4C). Finally, phosphorylation at Ser28 (peptide **47**)[19] reduced the inhibitor potency ~12-fold. These results demonstrate that PRC2 inhibition by K27M can be reduced through the deposition of specific histone PTMs within the same tail, in analogy to binary switches observed in many histone modification crosstalks.[20]

We were intrigued by the possibility that histone PTMs may also be able to detoxify the K27M mutation *in vivo*. This hypothesis is most easily tested for phosphoserine since this residue can be mimicked by a Ser to Glu mutation. *In vitro*, the K27Nle/S28E double mutant (peptide **48**) displayed reduced inhibitor potency compared to the K27Nle mutant (Figures 3A and S4B). To extend these results *in vivo*, we transduced HEK 293T cells with lentiviruses containing wild-type histone H3.3, K27M, S28E, or the double mutant K27M/S28E and compared the level of K27me2 and K27me3 in the resulting cell lines (Figures 3B and S4D). In agreement with our *in vitro* measurements, the phosphoserine-mimetic S28E partially rescued the formation of K27me2 and K27me3 modifications that are suppressed by the presence of K27M. These results argue that PTMs can strongly attenuate K27M-dependent loss of K27 methylation, perhaps contributing to the existence of K27me3-rich chromatin regions in K27M-containing tumors.

In summary, we have mapped the binding interaction between the histone methyltransferase PRC2 and cancer-derived H3K27M histone mutants. Potent inhibition relies on long, hydrophobic residues to interact with the lysine binding channel of the active site. The catalytic subunit, EZH2, recognizes the entire H3 tail, in particular regions surrounding residue 27 and the N-terminus. Interfering with these binding hotspots through PTMs attenuates inhibition, which suggests that modulating alternate chromatin modification pathways may provide a therapeutic strategy for K27M detoxification.

■ ASSOCIATED CONTENT

Supporting Information

Experimental procedures, analytical data, supporting schemes, and figures. Full citations for references 5, 6, 9, 11 and 17. This material is available free of charge via the Internet at http://pubs.acs.org.

■ AUTHOR INFORMATION

Corresponding Author

*muir@princeton.edu

Author Contributions

‖These authors contributed equally.

Notes

The authors declare no competing financial interest.

■ ACKNOWLEDGMENTS

We thank Lotus separations for purification of Fmoc-2-aminoheptanoic acid, Ha-Eun Kong for help with peptide synthesis, Dr. Lenka Bittova for providing p300, and members of the Muir and Allis laboratories for valuable discussions. This research was supported by the U.S. National Institutes of Health (grants R37-GM086868 and R01 GM107047) and the STARR foundation (grant I6-A614).

■ REFERENCES

(1) Strahl, B. D.; Allis, C. D. *Nature* **2000**, *403*, 41.
(2) Ciferri, C.; Lander, G. C.; Maiolica, A.; Herzog, F.; Aebersold, R.; Nogales, E. *Elife* **2012**, *1*, e00005.
(3) Simon, J.; Lange, C. *Mutat. Res.* **2008**, *647*, 21.
(4) Kuzmichev, A.; Nishioka, K.; Erdjument-Bromage, H.; Tempst, P.; Reinberg, D. *Genes Dev.* **2002**, *16*, 2893.
(5) Schwartzentruber, J.; Korshunov, A.; Liu, X. Y.; Jones, D. T.; Pfaff, E.; Jacob, K.; Sturm, D.; Fontebasso, A. M.; Quang, D. A.; Tonjes, M.; et al. *Nature* **2012**, *482*, 226.
(6) Wu, G.; Broniscer, A.; McEachron, T. A.; Lu, C.; Paugh, B. S.; Becksfort, J.; Qu, C.; Ding, L.; Huether, R.; Parker, M.; et al. *Nat. Genet.* **2012**, *44*, 251.
(7) Lewis, P. W.; Müller, M. M.; Koletsky, M. S.; Cordero, F.; Lin, S.; Banaszynski, L. A.; Garcia, B. A.; Muir, T. W.; Becher, O. J.; Allis, C. D. *Science* **2013**, *340*, 857.
(8) Chan, K.-M.; Fang, D.; Gan, H.; Hashizume, R.; Yu, C.; Schroeder, M.; Gupta, N.; Mueller, S.; James, C. D.; Jenkins, R.; Sarkaria, J.; Zhang, Z. *Genes Dev.* **2013**, *27*, 985.
(9) Bender, S.; Tang, Y.; Lindroth, A. M.; Hovestadt, V.; Jones, D. T.; Kool, M.; Zapatka, M.; Northcott, P. A.; Sturm, D.; Wang, W.; et al. *Cancer Cell* **2013**, *24*, 660.
(10) Lowary, P. T.; Widom, J. *J. Mol. Biol.* **1998**, *276*, 19.
(11) Diaz, E.; Machutta, C. A.; Chen, S.; Jiang, Y.; Nixon, C.; Hofmann, G.; Key, D.; Sweitzer, S.; Patel, M.; Wu, Z.; et al. *J. Biomol. Screen.* **2012**, *17*, 1279.
(12) Cheng, Y.; Prusoff, W. H. *Biochem. Pharmacol.* **1973**, *22*, 3099.
(13) Copeland, R. A. Reversible Inhibitors. In *Enzymes*; John Wiley & Sons, Inc.: Hoboken, NJ, 2002; pp 266−304.
(14) Trievel, R. C.; Beach, B. M.; Dirk, L. M.; Houtz, R. L.; Hurley, J. H. *Cell* **2002**, *111*, 91.
(15) Margueron, R.; Reinberg, D. *Nature* **2011**, *469*, 343.
(16) Margueron, R.; Justin, N.; Ohno, K.; Sharpe, M. L.; Son, J.; Drury, W. J., III; Voigt, P.; Martin, S. R.; Taylor, W. R.; De Marco, V.; Pirrotta, V.; Reinberg, D.; Gamblin, S. J. *Nature* **2009**, *461*, 762.
(17) Schmitges, F.; Prusty, A.; Faty, M.; Stützer, A.; Lingaraju, G.; Aiwazian, J.; Sack, R.; Hess, D.; Li, L.; Zhou, S.; et al. *Mol. Cell* **2011**, *42*, 330.
(18) Di Lorenzo, A.; Bedford, M. T. *FEBS Lett.* **2011**, *585*, 2024.
(19) Lau, P. N.; Cheung, P. *Proc. Natl. Acad. Sci. U.S.A.* **2011**, *108*, 2801.
(20) Fischle, W.; Wang, Y.; Allis, C. D. *Nature* **2003**, *425*, 475.